Renormalized Waves and Discrete Breathers in β-Fermi-Pasta-Ulam Chains

Boris Gershgorin,[1] Yuri V. Lvov,[1] and David Cai[2]

[1]*Department of Mathematical Sciences, Rensselaer Polytechnic Institute, Troy, New York 12180, USA*
[2]*Courant Institute of Mathematical Sciences, New York University, New York, New York 10012, USA*

(Received 3 June 2005; published 20 December 2005)

We demonstrate via numerical simulation that in the *strongly* nonlinear limit the β-Fermi-Pasta-Ulam (β-FPU) system in thermal equilibrium behaves surprisingly like weakly nonlinear waves in properly renormalized normal variables. This arises because the collective effect of strongly nonlinear interactions effectively renormalizes linear dispersion frequency and leads to effectively weak interaction among these renormalized waves. Furthermore, we show that the dynamical scenario for thermalized β-FPU chains is spatially highly localized discrete breathers riding chaotically on spatially extended, renormalized waves.

DOI: 10.1103/PhysRevLett.95.264302 PACS numbers: 45.05.+x, 05.20.−y, 05.45.−a

The Fermi-Pasta-Ulam (FPU) lattice was introduced in their classical work [1] to address fundamental issues of statistical physics such as equipartition of energy, ergodicity. The attempt to resolve the mystery of the FPU recurrence (the system did not thermalize as was expected but rather kept returning to the initial state [1]) has spurred many great mathematical and physical discoveries, such as the celebrated Kol'mogorov-Arnol'd-Moser theorem and soliton physics [2]. Despite this remarkable progress, there are still fundamental open questions that are under vigorous debate [3], such as what is the route to thermalization and how to fully characterize the thermalized β-FPU system. Furthermore, in the last decade discrete breathers (DBs) as spatially localized, time periodic lattice excitations were discovered [4]. Arising from energy localization in nonlinear lattices, they play important roles in fiber optics, condensed matter physics, and molecular biology [5]. The existence of DBs has been addressed rigorously [6]. Important conceptual issues naturally arise, such as what is the role of DBs on the route to equilibrium [7] and how do they manifest in thermalization of the FPU system? Resolution of these issues will certainly provide deep insight into the fundamental understanding of route to thermalization for general nonlinear physical systems. Most of the results regarding DBs in β-FPU chains have so far only addressed their behavior in the transient state of *weakly* nonlinear regimes before thermalization occurs [8,9].

In this Letter, we investigate the FPU dynamics in the strongly nonlinear limit. We demonstrate that, quite surprisingly, even for strong nonlinearity, the β-FPU system in thermal equilibrium behaves like weakly nonlinear waves in properly chosen variables. Such behavior results from the collective effect of strongly nonlinear interactions effectively renormalizing linear dispersion relation. This observation enables us to use a well-developed weak turbulence (WT) formalism [10] for the description of the β-FPU chains even in a strongly nonlinear regime. Furthermore, in addition to the nonlinear waves, we observe the DB excitations in the thermalized state of β-FPU chains. Previously such DBs were observed only during transient stages towards thermalization [8]. Here we show via numerical simulation that DBs actually persist and coexist with renormalized waves in the thermalized state. Thus, in the thermalized β-FPU, there are two kinds of quasiparticle excitations, one localized in k space as renormalized nonlinear waves or phonons, and the other localized in x space as DBs.

The β-FPU chain is described by the Hamiltonian

$$H = H_2 + H_4, \qquad H_2 = \frac{1}{2}\sum_{i=1}^{N} p_i^2 + (q_i - q_{i+1})^2, \qquad H_4 = \frac{\beta}{4}\sum_{i=1}^{N}(q_i - q_{i+1})^4, \tag{1}$$

with periodic boundary conditions, where β is *a nonlinear parameter* and p_i and q_i are the ith particle momentum and displacement from the equilibrium position, respectively. In terms of P_k and Q_k, the Fourier transforms of p_i and q_i, the Hamiltonian becomes

$$H = \frac{1}{2}\sum_{k=1}^{N-1}[|P_k|^2 + \omega_k^2|Q_k|^2] + V(Q), \tag{2}$$

where $\omega_k = 2\sin\frac{\pi k}{N}$ is the linear dispersion frequency and $V(Q)$ is the Fourier transform of H_4. $V(Q)$ is a linear combination of various quartic products of Q_k's and Q_k^*'s. We numerically integrate the canonical equations of motion for Hamiltonian (1) to study possible dynamical scenario of the FPU [11]. Since the thermalized state is our primary interest we chose random initial data [11]. Note that the behavior of the β-FPU in equilibrium is fully characterized by only one parameter βH [13] where H is the total energy of the system. We fixed $H = 200$ and $N = 128$ (except for Fig. 6, where $N = 1024$) and varied β.

First, for the FPU system in thermal equilibrium [14], with moderate and strong nonlinearities $\beta = 1$, 8, and 32, we measured the power spectrum $\langle|a_k|^2\rangle$ as a function of ω_k, where $a_k = (P_k - i\omega_k Q_k)/\sqrt{2\omega_k}$ and $\langle\cdots\rangle$ denotes the time averaging. Although it was expected that, for weak nonlinearity, $\langle|a_k|^2\rangle = T/\omega_k$, where T is an effective temperature (Rayleigh-Jeans distribution for waves [10]),

it is surprising to find that the same scaling holds even for strong nonlinearities as shown in Fig. 1. To understand why $\langle |a_k|^2 \rangle$ scales as ω_k^{-1} even in the strongly nonlinear limit, we computed the ω-k spectrum of $a_k(t)$ as shown in Fig. 2(a). In the weakly nonlinear limit the spectrum would have resonant peaks along a curve given by the linear dispersion relation $\omega_k = 2\sin(k\pi/N)$. We observe that, when the nonlinearity is no longer small, the resonances move to higher frequencies, as the dispersion relation is renormalized by the nonlinear part $V(Q)$. The renormalized dispersion relations is indicated by the sinelike structure of the resonance peaks [the solid line in Fig. 2(a)]. We verified numerically that the main contribution of the nonlinear potential energy ($\sim$80%) comes from the terms $Q_k Q_l Q_m^* Q_s^*$ constrained on $k + l = m + s$. We note that when $k = m$ and $l = s$ or $k = s$ and $l = m$, these terms can be combined with the quadratic part of (2) to effectively renormalize the frequency ω_k. More specifically, Hamiltonian (2) can be rewritten as the sum of a new renormalized quadratic part and a remaining nonlinear part: $H = \tilde{H}_2 + \tilde{H}_4$, where $\tilde{H}_2 = \frac{1}{2}\sum_{k=1}^{N-1}(|P_k|^2 + \tilde{\omega}_k^2 |Q_k|^2)$ with the renormalized dispersion relation

$$\tilde{\omega}_k = \eta \omega_k, \qquad \eta = \sqrt{1 + \frac{3\beta}{2N} \sum_{l=1}^{N-1} \langle |Q_l(t)|^2 \rangle \omega_l^2}. \quad (3)$$

Note that the frequency renormalization factor η does not depend on k. Figure 2(b) shows how the renormalized frequency $\tilde{\omega}_k$ depends on β. The upper curve was produced from the numerical spectrum—the abscissas of the peaks of the sinelike curves were measured [e.g., from Fig. 2(a) for $\beta = 1$, $\omega_{k=N/2} = 3.3$ for $N = 128$]. The curve with pluses was obtained using Eq. (3). Both seem to possess a scaling $\sim \beta^{0.2}$ dependence [see Fig. 2(b)]. The discrepancy between the analytical and numerical curves can be attributed to the fact that in the derivation of (3) we took into account only 4-wave processes. In principle, we can take into account higher order processes to obtain a more accurate analytical estimate of η.

To further study the renormalization of interactions we measured the ratio of the quartic to the quadratic parts of the energy *before* and *after* renormalization procedure (i.e., H_4/H_2 vs $\tilde{H}_4/\tilde{H}_2$) for different values of β with energy fixed [Fig. 2(c)]. This figure also shows that the effective renormalized linear part becomes more dominant. Therefore, even for strongly nonlinear regimes, with β as large as 128, the *renormalized waves* (or purely nonlinear phonons) have weakened interactions. Note that the resonance of $a_k(\omega)$ has a finite width [shown with the dashed lines in Fig. 2(a), which are the level of $\int |a_k|^2(\omega) d\omega / \max_\omega |a_k|^2$ for each k]. Note that for $k = N/2$ (the highest mode in the system) the resonances become the broadest. According to WT [10], the energy exchange among waves occurs on the resonance manifold given by $k_1 + k_2 = k_3 + k_4$ and $\omega_{k_1} + \omega_{k_2} = \omega_{k_3} + \omega_{k_4}$. Although one can show that there are no exact resonances in β-FPU chains on the discrete lattice, the nonlinearity induced near resonance interactions (i.e., $|\omega_{k_1} + \omega_{k_2} - \omega_{k_3} - \omega_{k_4}| < \delta$, where δ is a resonance width) can occur. This allows us to use the WT theory if the interaction is considered to be weak. In order to characterize the system as weakly nonlinear waves, the renormalized waves are described by the new normal variables $\tilde{a}_k = (P_k - i\tilde{\omega}_k Q_k)/\sqrt{2\tilde{\omega}_k}$. The relationship between bare a_k and renormalized $\tilde{a}_k$ is $a_k = [(\sqrt{\eta} + 1/\sqrt{\eta})\tilde{a}_k + (\sqrt{\eta} - 1/\sqrt{\eta})\tilde{a}_{-k}^*]/2$. Under the random phases approximation [16] for a_k we have $\langle |\tilde{a}_k|^2 \rangle = 2\eta/(1 + \eta^2)\langle |a_k|^2 \rangle$. Therefore the power spectrum has scaling ω_k^{-1} for both a_k and $\tilde{a}_k$. (Note that $\langle |a_k|^2 \rangle$ is shown in Fig. 1.) As a consequence, the effective temperature, $\tilde{T}$, for the renormalized waves is related to the bare temperature T by $\tilde{T} = [2\eta^2/(1 + \eta^2)]T$.

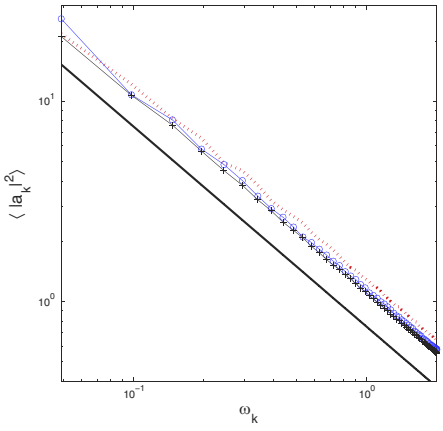

FIG. 1 (color online). Power spectra for the thermalized state for relatively strong nonlinearity $\beta = 1$ (dots), $\beta = 8$ (circles), and $\beta = 32$ (pluses). The thick solid line is $1/\omega_k$. Time window $T = 10^5$ was used for averaging the power spectrum.

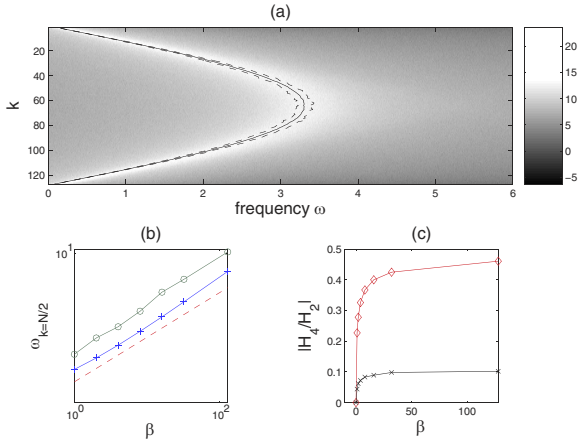

FIG. 2 (color online). (a) Density plot of spectrum for $\beta = 1$ and $H = 200$ [$\ln(|a_k(\omega)|^2)$ is plotted]. (b) Renormalized linear frequency as a function of β: analytical predictions (pluses) and numerical measurements (circles). $\beta^{0.2}$ is shown for comparison (dashed line). (c) Effective nonlinearity as a function of β before (diamonds) and after (crosses) renormalization.

The renormalization picture is further corroborated by the time evolution of each individual wave $\tilde{a}_k$. For the bare waves a_k, there are large temporal modulations in both modulus and phase as a result of strong nonlinear interaction among these modes on the linear dispersion time scale [as shown in Figs. 3(a) and 3(b)]. In weakly nonlinear systems, wave amplitudes and corresponding phases are expected to evolve slowly on the linear dispersion time scale. For renormalized waves [Figs. 3(c) and 3(d)] these modes indeed have characteristics of weakly interacting waves, with a small modulation in $|\tilde{a}_k|^2$ and phase.

Now we turn to the numerical evidence for the persistence of DBs in the thermalized β-FPU chain. As observed before [8], there are DBs present in the transient state. As nonlinearity increases, the duration of transient becomes shorter. After the energy redistributes among all the modes to achieve thermal equilibration, our simulations show that the spatially localized, high frequency excitations still exist. These DBs can interact with each other and may be destroyed by collision processes with other DBs or with the renormalized waves. The spatial structure of these excitations very much resembles the idealized breather oscillations in the absence of spatially extended waves: they ''live'' above the high frequency edge of the dispersion band and their lifetime is sufficiently long (on the order of 10–100 DB oscillations) to behave like a quasiparticle. Note that, under certain conditions, supersonic solitons may arise from the β-FPU system as another kind of localized excitations [17,18]. However, they were not observed in our thermalized system. Figure 4 is the energy density plot which shows the time evolution of energy of each particle for the transient (recording starting time $T_0 = 5 \times 10^2$) and thermalized ($T_0 = 5 \times 10^5$) states, respectively. Figures 4(c) and 4(d) display the energy as a function of site at T_0 corresponding to Figs. 4(a) and 4(b), respectively. In the transient case [Fig. 4(a)] the spatially localized objects (dark stripes) that carry sufficiently large amount of energy are clearly observed. Figure 4(c) is a snapshot of the energy density plot [Fig. 4(a)] at T_0. Here the DBs are seen as localized peaks [8]. After thermalization the spatial structure looks different [Fig. 4(b)]. The system now consists of the renormalized waves [straight crosshatch traces in Fig. 4(b)]. On the top of these waves, the localized structures similar to DBs manifest themselves as the wavy dark trajectories [in Fig. 4(b)]. Although the snapshot [Fig. 4(d)] of the energy density plot [Fig. 4(b)] indicates that in thermal equilibrium the energy is more evenly distributed among particles, spatially localized structures are clearly observed.

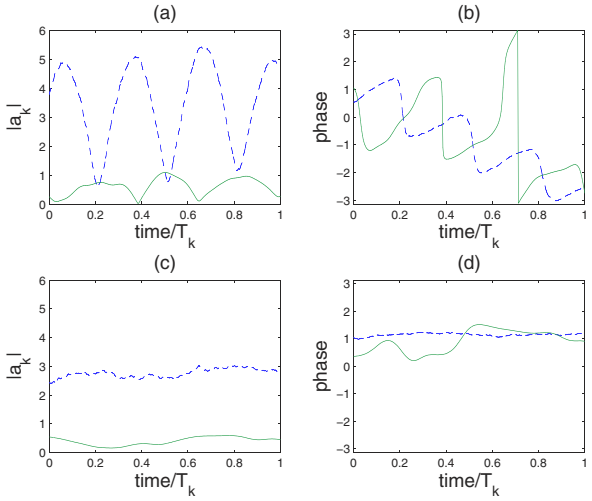

FIG. 3 (color online). (a),(b) $|a_k|$ and phase, respectively, using the bare linear dispersion $\omega_k = 2\sin(\pi k/N)$. (c),(d) $|\tilde{a}_k|$ and phase, respectively, using the renormalized dispersion $\tilde{\omega}_k$ [Eq. (3)]. Dashed lines, $k = 1$; solid lines, $k = 20$. The dispersion time scale is described by $T_k = 2\pi/\omega_k$ for panels (a) and (b), and $T_k = 2\pi/\tilde{\omega}_k$ for panels (c) and (d). (Note that, since $a_k = |a_k|e^{i(\phi+\omega_k t)}$, the phase excludes the linear rotation.)

Since there are renormalized waves in the system, which also carry energy, we need to find a way to distinguish between these waves and DBs. We use a frequency filter that cuts out the lower side of the Fourier spectrum and leaves the high frequency part unmodified, i.e., $f(g(n,t)) = \mathrm{Re}F^{-1}(H_\omega(F(g)))$, where Re denotes the real part, F is a time Fourier transform, H_ω eliminates all frequencies below ω_{cut}, and $g(n,t)$ is a dynamical variable that is being filtered. By applying this filter to the displacement q_n to obtain $q_n^f \equiv f(q_n)$, we can show the existence of DBs even for strong nonlinearities, for example, $\beta = 25$. Figure 5(a) shows a clear example of a DB excitation reconstructed using the filtered q_n^f with $\omega_{\mathrm{cut}} = 7$. Figure 5(b) shows a typical spatial profile of the DB taken from Fig. 5(a), which strongly resembles the idealized DB [19]. Finally, in Fig. 6, we present the evidence that there is a *turbulence* of DBs, which chaotically ride on renormalized waves. The corresponding energy density distribution along with the distri-

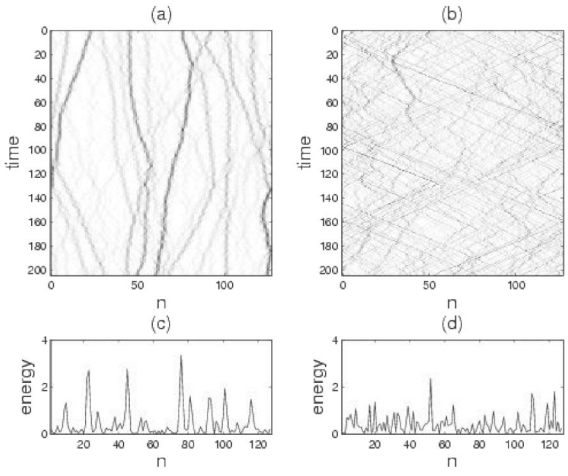

FIG. 4. Energy density evolution of (a),(c) the transient state and (b),(d) the thermalized state ($\beta = 1$ and $H = 200$). In (a) and (b) the darker strips correspond to high energy localizations; (c) and (d) are the snapshots of energy density.

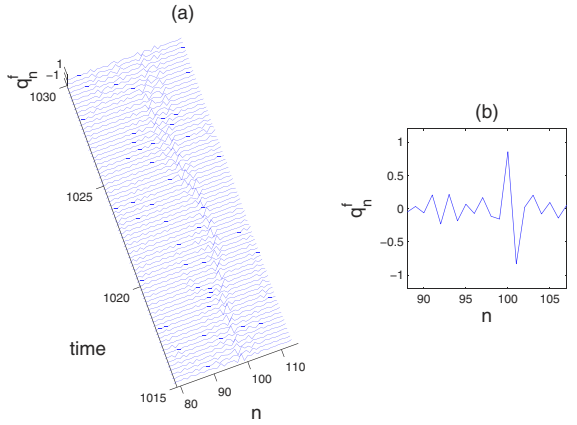

FIG. 5 (color online). (a) Evolution of a discrete breather in thermal equilibrium. (b) Typical snapshot of the breather. $\beta = 25$; $H = 200$.

bution of filtered displacement in a zoomed region $q_n^f(t)$ is displayed in Figs. 6(a) and 6(b), respectively. After the lower modes from the displacement q_n are filtered, one can clearly observe that the remaining high frequency oscillations are spatially highly localized, with the same characteristics as an idealized breather. The detailed time dynamics of the DB shows the main characteristics of breathers: the values of q_n^f change signs periodically (as indicated by the alternating white and black spots along the trajectory) as the DB moves in space, with a spatial span of 2 or 3 sites only, as seen in Fig. 6(b).

In conclusions, we have presented an interesting dynamical scenario of the β-FPU chains in thermal equilibrium: (i) For strong nonlinearity the linear dispersion relation is effectively renormalized, which allows one to treat even strongly nonlinear systems as if they were weakly nonlinear. (ii) On top of renormalized waves, the strongly nonlinear system is also characterized by the turbulence of discrete breathers.

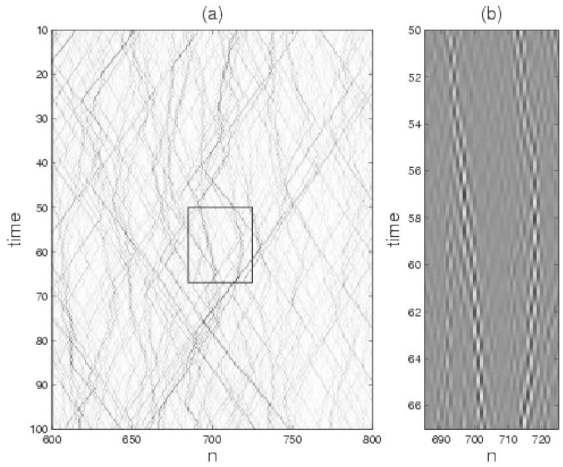

FIG. 6. Turbulence of discrete breathers ($N = 1024$): (a) evolution of energy density; (b) zoomed in $q_n^f(t)$ of the area indicated by the rectangle in (a).

We thank Sergei Nazarenko for discussions, and NSF DMS 0134955 (Y. L.) and NSF DMS 0206779 (D. C.) for support.

[1] E. Fermi, J. Pasta, and S. Ulam, Los Alamos Scientific Laboratory Report No. LA-1940 (reprinted in *Fermi E. Collected Papers* by University of Chicago Press, Chicago, 1965, Vol. II, p. 978).
[2] J. Ford, Phys. Rep. **213**, 271 (1992); M. Toda, *Theory of Nonlinear Lattice* (Springer-Verlag, New York, 1989).
[3] A. Carati, L. Galgani, and A. Giorgilli, Chaos **15**, 015105 (2005), and references therein.
[4] S. Flach and C. R. Willis, Phys. Rep. **295**, 181 (1998), and references therein; J. Szeftel *et al.*, Physica (Amsterdam) **181D**, 215 (2003).
[5] M. Eleftheriou and S. Flach, Physica (Amsterdam) **202D**, 142 (2005); C. H. Choi *et al.*, Nucleic Acids Res. **32**, 1584 (2004).
[6] S. Aubry, G. Kopidakis, and V. Kadelburg, Discrete Contin. Dyn. Syst. B **1**, 271 (2001); G. James, C. R. Acad. Sci., Ser. I, Math. **332**, 581 (2001).
[7] T. Dauxois, S. Ruffo, and A. Torcini, Phys. Rev. E **56**, R6229 (1997); K. Aoki and D. Kuznezov, Phys. Rev. Lett. **86**, 4029 (2001); H. Zhao *et al.*, *ibid.* **94**, 025507 (2005).
[8] T. Cretegny *et al.*, Physica (Amsterdam) **121D**, 109 (1998).
[9] L. S. Schulman *et al.*, Phys. Rev. Lett. **88**, 224101 (2002); M. Kastner, Phys. Rev. Lett. **92**, 104301 (2004).
[10] V. E. Zakharov, V. S. Lvov, and G. Falkovich, *Kolmogorov Spectra of Turbulence* (Springer-Verlag, Berlin, 1992).
[11] We have verified that neither the choice of various integrators nor the initial conditions of spatially random or regular structures affect the reported results. We used the sixth order Yoshida algorithm [12], a second order symplectic and adaptive Runge-Kutta integrators. We ensured a high degree of accuracy; e.g., the energy is conserved up to the ninth digit for a runtime $T = 10^6$.
[12] H. Yoshida, Phys. Lett. A **150**, 262 (1990).
[13] P. Poggy and S. Ruffo, Physica (Amsterdam) **103D**, 251 (1997).
[14] To confirm that the system had reached the thermal equilibrium we monitored $C(t) = N(\sum E_i^2)/(\sum E_i)^2$ where E_i is the energy of the ith particle [8]. The value of $C(t)$ is $O(N)$ when all the energy is concentrated around one site and is $O(1)$ when equipartition is reached. And $C(t)$ had values in the range 1–3 in our simulations. Also various statistics of the system were verified to ensure that it reached the thermalized state with the Gibbs distribution [15]: (i) p_i of each particle distributed with $P(p) \sim e^{-p^2/(2T)}$, and (ii) $y_i = q_i - q_{i-1}$ distributed with $P(y) \sim e^{-(y^2/2+\beta y^4/4)/T}$.
[15] L. Landau and E. Lifshitz, *Statistical Physics*, Course of Theoretical Physics Vol. 5 (Pergamon, Oxford, 1958).
[16] Y. Lvov and S. Nazarenko, Phys. Rev. E **69**, 066608 (2004).
[17] Yu. A. Kosevich *et al.*, Europhys. Lett. **66**, 21 (2004).
[18] F. Zhang *et al.*, Phys. Rev. E **61**, 3541 (2000).
[19] Y. Kivshar *et al.*, Phys. Rev. B **58**, 5423 (1998).